

Coupled spin-boson systems far from equilibrium

M. I. Salkola

Department of Physics, Stanford University, Stanford, California 94305

A. R. Bishop

Theoretical Division, Los Alamos National Laboratory, Los Alamos, New Mexico 87545

V. M. Kenkre and S. Raghavan

Center for Advanced Studies, University of New Mexico, Albuquerque, New Mexico 87131

(Received 22 July 1996)

Nonequilibrium quantum dynamics of a system comprising a (pseudo) spin- $\frac{1}{2}$ object coupled to a boson degree of freedom is studied. It is shown that the time evolution of the system is described by a set of elementary scattering processes. Through these processes the system approaches an equilibrium in which the spin is in a mixed state that on average maximizes its entropy. However, the irregular behavior of the system is unrelated to “quantum chaos” as the Hamiltonian is integrable. [S0163-1829(96)51042-8]

In studies of systems describing quasiparticles moving on a lattice and interacting with boson degrees of freedom, the emphasis is, in general, on their low-energy properties, such as polaron formation and dynamics. These model studies provide important insights in many cases for an understanding of dynamic correlations near thermodynamic equilibrium. Equally important are situations where the system is driven far from its equilibrium state. In particular, these situations provide useful information on many-body interactions and correlation effects that at low energies can be strongly renormalized. While much of the interpretation of physically interesting and important systems relies on effective Hamiltonians at a specific energy scale, experimental probes can now perturb these systems in a wide range of energies, as a result of the advent of, e.g., intense laser sources. This provides a clear impetus for exploring the dynamics at higher energies, because the behavior of the system and the experimental manifestations can be strongly scale dependent.

Here, we consider the dynamics of the spin boson model with spin- $\frac{1}{2}$, described by the Hamiltonian

$$H = -V\sigma_1 + \lambda\hat{\phi}\sigma_3 + \frac{1}{2}\epsilon_0(\hat{\pi}^2 + \hat{\phi}^2), \quad (1)$$

where σ_a ($a=1,2,3$) are the three Pauli operators, $[\sigma_a, \sigma_b] = 2i\sigma_c$ (a,b,c cyclic). The two-site Holstein Hamiltonian¹ can be cast into the above form by defining the Pauli operators in terms of the quasiparticle operators as $\sigma_1 = c_1^\dagger c_2 + c_2^\dagger c_1$, $\sigma_2 = -i(c_1^\dagger c_2 - c_2^\dagger c_1)$, and $\sigma_3 = c_1^\dagger c_1 - c_2^\dagger c_2$. Here, $\{c_k, c_l^\dagger\} = \delta_{kl}$ ($k,l=1,2$). The dimensionless conjugate operators ϕ and π , obeying the commutation relation $[\hat{\phi}, \hat{\pi}] = i$, describe a boson degree of freedom with energy ϵ_0 . The spin tends to precess about the σ_1 axis with the rate determined by V (>0). At the same time, it interacts with the boson mode ϕ , the interaction strength being specified by the coupling constant λ .

This spin-boson model has been the subject of intensive attention because of its relevance to quasiparticle-phonon systems¹ and to the interaction of light with matter.² It is capable of describing polaron formation and dynamics, cor-

relation effects, and experimental observables in highly nonlinear and nonadiabatic systems. Because of the model’s importance to many physically interesting cases, various approximative approaches are used for solving the problem, most notably the semiclassical approximation³⁻⁵ and the rotating-wave approximation.^{2,6} Recently, it has also been studied by exact diagonalization,^{3,7-9} focusing on the collective, multitime scale behavior of the coupled degrees of freedom and the validity of approximative schemes.

The noninteracting problem ($\lambda=0$) is characterized by two time scales: the spin period $\tau_S = \pi/V$ and the boson period $\tau_B = 2\pi/\epsilon_0$. At low energies, with increasing λ/ϵ_0 , the quantum dynamics leads to the formation of a new composite particle, the polaron, where the motion of the spin is slaved to the boson dynamics. A characteristic signature of this nonlinear dynamics is the appearance of a very long time scale $\tau_T = \pi/\epsilon_T$, corresponding to the reduced polaron bandwidth ϵ_T ; see Fig. 1. The questions concerning the coherence and particlelike nature of the polaronic excitations and

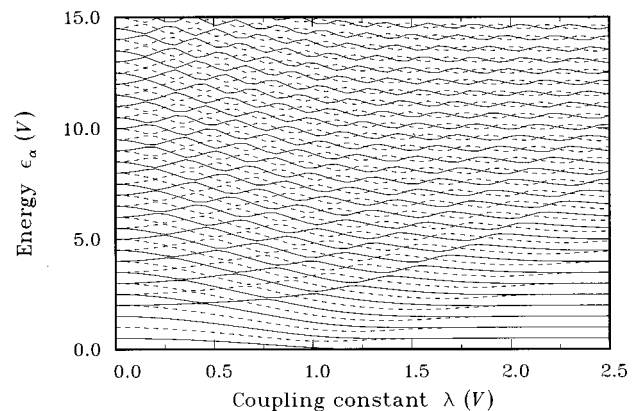


FIG. 1. The energy spectrum relative to the ground state of the spin-boson Hamiltonian (1) as a function of λ for $\epsilon_0/V=1/2$. The even and odd parity states are shown as dashed and solid lines, respectively.

the effect of quantum and thermal fluctuations is of great interest. Our goal is to explore these questions in terms of Husimi distribution functions.¹⁰ These lead to a pictorial description of polaron dynamics which, for example, explains the loss of coherence and composite nature of the polaron. The quantum evolution of the spin-boson system is computed based on accurate numerical diagonalization^{9,11} of Hamiltonian (1).

The Husimi distribution functions¹⁰ are conveniently defined in terms of reduced density operators:

$$\rho_B(\tau) = \text{Tr}_S \rho(\tau), \quad (2a)$$

$$\rho_S(\tau) = \text{Tr}_B \rho(\tau); \quad (2b)$$

where B and S denote the boson and spin subsystems, respectively. The density operator for the full system is

$$\rho(\tau) = |\Psi(\tau)\rangle\langle\Psi(\tau)|, \quad (3)$$

where $|\Psi(\tau)\rangle$ is the state of the system at time τ : $|\Psi(\tau)\rangle = e^{-iH\tau}|\Psi_0\rangle$. Here, $\tau = t/\hbar$ is the scaled time and $|\Psi_0\rangle$ is the initial state at $\tau=0$. Often, these reduced density operators have a property that $\langle\rho_A(\tau)\rangle \equiv \text{Tr}\rho_A^2(\tau) \neq 1$ ($A=B,S$): the dynamics leads to a mixed state for a subsystem because of the coupling. For the spin subsystem, bounds can be established: $\frac{1}{2} \leq \langle\rho_S\rangle \leq 1$. By virtue of the relation, $\langle\rho_S\rangle = (\langle\vec{\sigma}\rangle^2 + 1)/2$, complete mixing also implies a vanishing Bloch vector $\langle\vec{\sigma}\rangle$.¹² Here, $\vec{\sigma}$ is a vector whose components are the Pauli matrices σ_a . In contrast, in the semiclassical approximation, the degree of mixing, as measured by $\langle\rho_S\rangle$ and the length of the Bloch vector, becomes a constant of motion. We can also formally consider the Gibbs entropy for a subsystem A , defined as $S_A = -\text{Tr}\rho_A \ln \rho_A$ ($A=B,S$). For a closed system in a pure state, $S_A \equiv 0$. While in the absence of interactions to the environment (e.g., with the bath), the entropy of the coupled system is a constant of motion, the entropy of a subsystem usually is not. For example, S_S will reflect the degree of mixing of the spin (quasiparticle) state.

We focus on the Husimi distribution because of its correspondence with the coarse-grained classical distribution function and because it does not share the well-known inconvenient characteristics of the Wigner distribution that it is not positive-definite, rapidly oscillating, and can have large weight in a classically forbidden region. The Husimi distribution function is obtained by smoothing the corresponding Wigner distribution with a Gaussian. In the boson case, it has a simple formula:

$$\mathcal{H}_B(\pi, \varphi; \tau) = \langle z | \rho_B(\tau) | z \rangle, \quad (4)$$

where $|z\rangle = e^{z\hat{a}^\dagger - z^* \hat{a}} |0\rangle$ is the boson coherent state, $z = (\varphi + i\pi)/\sqrt{2}$, and $a = (\hat{\varphi} + i\hat{\pi})/\sqrt{2}$. In our numerical examples, the initial state is chosen to be a direct product of spin and boson coherent states:

$$|\Psi_0\rangle = |\eta_0\rangle \otimes |z_0\rangle, \quad (5)$$

where the coherent state for the spin is $|\eta_0\rangle = e^{\eta_0 \sigma_+ - \eta_0^* \sigma_-} |-\frac{1}{2}\rangle$, with $\sigma_\pm = (\sigma_1 \pm i\sigma_2)/2$ and $\eta_0 = (\theta_0/2)e^{-i\phi_0}$. Note that $0 \leq \theta_0 \leq \pi$ and $0 \leq \phi_0 < 2\pi$. The boson is in the coherent state, $\langle\varphi|z_0\rangle = \pi^{-1/4} e^{-(\varphi - \varphi_0)^2/2}$,

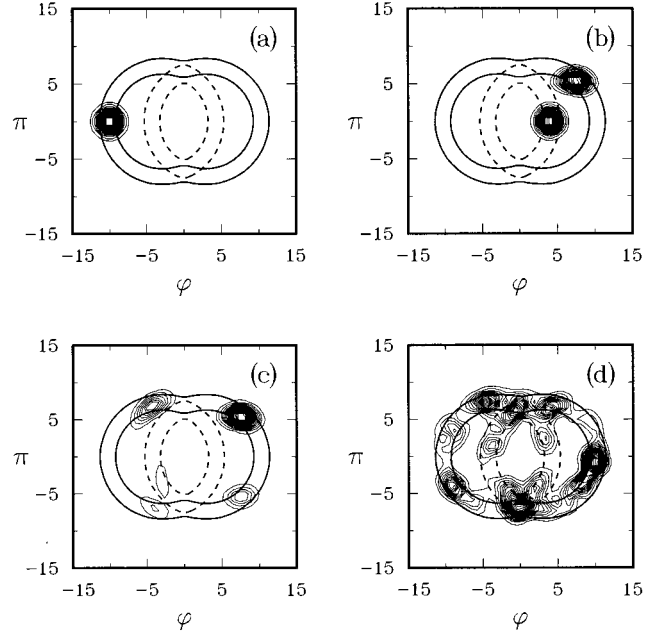


FIG. 2. The Husimi distribution $\mathcal{H}_B(\pi, \varphi; \tau)$ on the phase plane (π, φ) for times (a) $\tau=0$, (b) $\tau=\tau_B/2$, (c) $\tau=3\tau_B/2$, and (d) $\tau=\tau_T$, where $\tau_B=2\pi/\epsilon_0$ is the boson period and $\tau_T \approx 496.4\tau_B$ is the tunneling time. The constant-energy contours of $\epsilon_-(\pi, \varphi)$ and $\epsilon_+(\pi, \varphi)$ are denoted by heavy solid and dashed lines, respectively. Here, $\epsilon_0/V=1/2$ and $\lambda/V=3/2$. The system is initially in the product state (5) with $\varphi_0 = -10$.

with $z_0 = \varphi_0/\sqrt{2}$. Here, φ_0 is the average initial displacement of the boson coordinate and the spherical coordinates (θ_0, ϕ_0) give the average initial orientation of the spin. Since here we are mostly interested in large negative values of φ_0 , we choose $\theta_0 = \pi$ and $\phi_0 = 0$, yielding $|\eta_0\rangle = |\frac{1}{2}\rangle$.¹⁴ Figure 2 shows the Husimi distribution \mathcal{H}_B at various times for $\varphi_0 = -10$, which corresponds to the energy $\epsilon = 12.4 V$ (relative to the ground state). The spread of \mathcal{H}_B in time indicates a dispersing wave packet (loss of coherence).

In interpreting the above Husimi distributions, it is useful to generalize the result that applies for systems with one degree of freedom: \mathcal{H}_B is localized in the neighborhood of the constant-energy contour at ϵ , where ϵ is the energy of the initial state.¹³ Defining the adiabatic energy manifolds as

$$\epsilon_\pm(\pi, \varphi) = \frac{1}{2}\epsilon_0(\pi^2 + \varphi^2) \pm \sqrt{V^2 + (\lambda\varphi)^2}, \quad (6)$$

we should expect that, in the adiabatic regime, the Husimi distribution is localized in the neighborhood of the constant-energy contour $\epsilon = \epsilon_-(\pi, \varphi)$. In the high energy regime, where the initial wave packet has a large energy ϵ compared to the tunneling barrier, nonadiabatic corrections are important, and the problem reduces to that of rapid passage through a resonance, where the constant-energy contours of the Hamiltonian with $V=0$ are also important. These contours are determined by the functions

$$\tilde{\epsilon}_\pm(\pi, \varphi) = \frac{1}{2}\epsilon_0(\pi^2 + \varphi^2) \pm \lambda\varphi. \quad (7)$$

The signature of the composite nature of the polaron is that most of the density is localized for all times in phase space characterized by the lowest-energy adiabatic manifold,

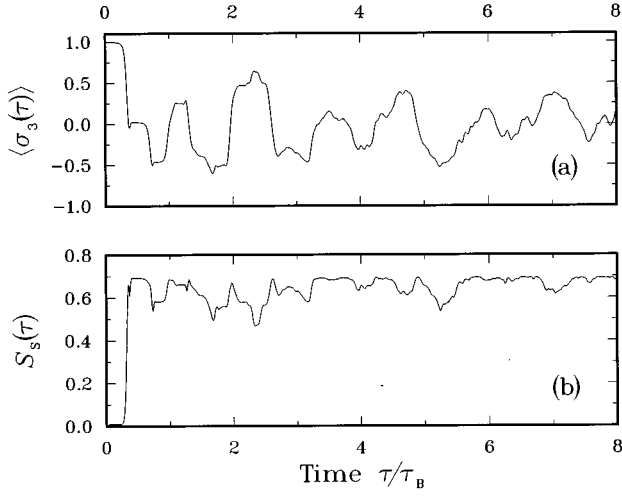


FIG. 3. The time evolution of (a) the spin component $\langle \sigma_3(\tau) \rangle$ and (b) the entropy $S_S(\tau)$ for the spin-boson model with $\epsilon_0/V=1/2$ and $\lambda/V=3/2$. The spin-boson system is initially in the product state (5) with $\varphi_0=-10$.

$\epsilon_-(\pi, \varphi)$. At low initial energies, the polaron mostly experiences processes in which part of it is transmitted through the tunneling barrier, and part is reflected, but which do not transfer any weight away from the lower adiabatic manifold. The increased initial energy leads to enhanced tunneling rates. In contrast, at much higher initial energies, the polaron begins to break down: each time the wave packet collides with the resonance region/tunneling barrier at $\varphi \sim 0$, it scatters mostly to the phase space region determined by the manifold $\epsilon \sim \epsilon_+(\pi, \varphi)$ and leave only a small portion on the adiabatic manifold. This behavior is illustrated in Fig. 2, where also the constant-energy contours of $\epsilon_{\pm}(\pi, \varphi)$ are depicted. The relative importance of these two scattering channels is determined by the energy of the initial state. This behavior is in striking contrast with that found in the Jaynes-Cummings model,¹⁵ which is obtained from the spin-boson Hamiltonian by the rotating-wave approximation. The difference arises because the rotating-wave approximation destroys the resonance regions that lead to the scattering events. These regions are located in phase space about the points where the energy manifolds $\tilde{\epsilon}_{\pm}(\pi, \varphi)$ intersect. However, for the Jaynes-Cummings model, the corresponding functions are concentric circles: $\tilde{\epsilon}_{\pm}(\pi, \varphi) = \frac{1}{2}\epsilon_0(\pi^2 + \varphi^2) \pm \lambda\sqrt{\pi^2 + \varphi^2}$.

For large displacements φ_0 , the boson component contains so much energy that it gains classical features. More precisely, in the limit $\varphi_0 \rightarrow -\infty$ and $\lambda \rightarrow 0$ with $\Lambda \equiv -\lambda\varphi_0 = \text{const}$,¹⁶ the dynamics of the spin variable is mapped to a time-dependent Landau-Zener problem,¹⁷ which is described by the time-dependent spin Hamiltonian, $H_S = -V\sigma_1 - \Lambda\sigma_3 \cos \epsilon_0\tau$. For $\Lambda \gg V$, the spin experiences kicks of the duration of $\tau_0 \approx (V/\pi\Lambda)\tau_B$, separated by half of a boson period. For $\tau_0 \ll \tau_S$, kicks are short, which leads to a steplike structure in $\langle \sigma_3(\tau) \rangle$. It is easy to see that, after the first kick, $\langle \sigma_3 \rangle$ is changed by an amount

$$\delta\langle \sigma_3 \rangle \approx \pi^2(\tau_0/\tau_S). \quad (8)$$

Figure 3 shows $\langle \sigma_3 \rangle$ as a function of time with those param-

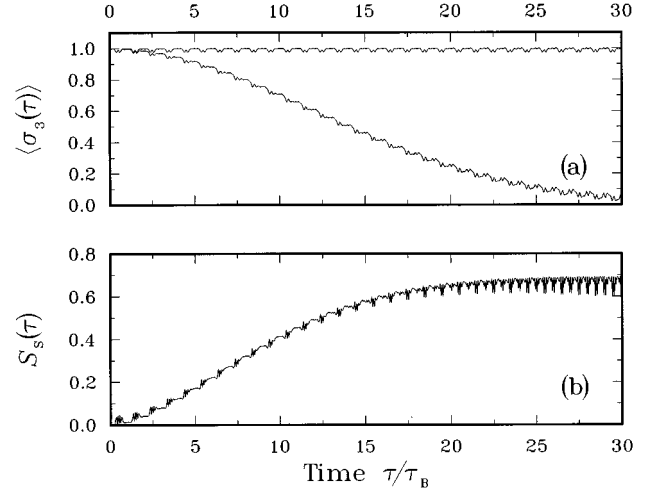


FIG. 4. (a) The time evolution of the spin component $\langle \sigma_3(\tau) \rangle$ as determined by the spin-boson Hamiltonian H (lower curve) and by the time-dependent spin Hamiltonian H_S (upper curve) for $\epsilon_0/V=10$ and $\lambda/V=1.3800195$. The spin-boson system is initially in the product state (5) with $\varphi_0=-20$. Thus, $2\Lambda/\epsilon_0$ is the second zero of the Bessel function J_0 . (b) Also shown is the entropy of the spin subsystem $S_S(\tau)$.

eters used in Fig. 2. The steplike structure is clearly visible at short times (a few phonon periods), and, for the first step, the estimate $\delta\langle \sigma_3 \rangle \approx 0.84$ given by Eq. (8) is close to the exact numerical value. During the time when the spin experiences a kick, the boson wave packet splits. For finite φ_0 , the energy stored in the boson degree of freedom is finite and its dynamics is affected by the spin-boson interaction. After sufficiently many splittings, the time evolution of the boson deviates from that of a free oscillator. In the example studied here, it happens already after a few phonon periods (see Fig. 3).

The time-dependent spin Hamiltonian H_S shows dynamical localization whenever parameters are such that the condition $J_0(2\Lambda/\epsilon_0)=0$ is fulfilled.¹⁸ Since the spin state becomes gradually mixed, we expect that dynamical localization will also eventually break down. This expectation is verified in Fig. 4. However, in the classical localization regime, the mixing occurs at a much slower rate for the spin (smaller rate of entropy production). This implies that, in the dynamical-localization regime, the qualitative dynamics of the spin is described by H_S for longer times because the tendency towards localization suppresses mixing of the spin state. The dynamics given by the Hamiltonian H_S deviates from that of H , once the entropy of the spin subsystem becomes large enough, i.e., $S_S \sim \ln 2$; see Figs. 3 and 4. In this context, it is worth emphasizing that the semiclassical dynamics in general must eventually deviate from the full quantum dynamics because the semiclassical dynamics generates no entropy per subsystem.

Our choice of the initial state, Eq. (5), guarantees that it is pure. When the main interest is in the low-energy phenomena, the boson part of the initial state is chosen so that $\langle \hat{\varphi} \rangle \sim -\lambda/\epsilon_0$.⁹ On general grounds, we may expect that the purity of the spin state is most susceptible to the spin-boson interaction during the tunneling event. Indeed, the exact nu-

merical calculation shows that $\langle \rho_S(\tau) \rangle$ has its lowest value there. Furthermore, in cases where the tunneling time τ_T is the longest one, the degree of pureness of the spin state is already affected at much shorter time scales. This time scale is connected to the revival time $\tau_\Delta \sim \tau_B$. For instance, the fast oscillations of quantum recurrences signify a nearly pure state (small entropy).¹⁹ The incomplete revivals can be interpreted as a partial loss of information due to quantum or thermal fluctuations. At nonzero temperatures, mixing becomes stronger and coherence (as associated with oscillations characteristic of a pure state) is reduced.²⁰ In other words, the boson-spin interaction causes incoherent motion of the polaron. This also implies a nearly vanishing Bloch vector $\langle \vec{\sigma} \rangle$.

We note that not only a strongly interacting system leading to a dynamic double well has interesting effects, but also that in a weakly interacting system a dispersing wave packet is observed. This is a result of repeated spin-boson collisions. Here, the boson propagation shows the loss of coherence due to quantum fluctuations. A similar phenomenon also occurs in the strongly interacting system even if the motion of the wave packet is confined to one of the wells because the well provides a nonlinear potential.

Even though the time-dependent Husimi distribution shows complicated behavior, it cannot be taken as an indication of “quantum chaos” on the basis of ideas from random-matrix theory where universal features of quantum spectra for classically chaotic systems are taken as evidence for complexity in the corresponding quantum systems. This complexity, often designated “quantum chaos,” is usually analyzed in terms of distributions of nearest-neighbor level

spacings²¹ and level curvatures²² as a function of a nonintegrability parameter. For example, for chaotic systems, the distribution for the nearest-neighbor level spacing Δ should have the form $\mathcal{P}(\Delta) \sim \Delta^\beta$ ($\beta=1,2,4$), for small Δ . The energy spectrum of the Hamiltonian (1) has numerous avoided level crossings, but there exists a nonzero energy scale Δ_0 below which no level spacings are found. This result is in accordance with the fact that the Hamiltonian is quantum integrable.²³ In addition to energy conservation, the system has inversion symmetry. The Hamiltonian can therefore be block diagonalized in terms of the parity operator, $P = e^{i\pi a^\dagger a} \otimes e^{i(\pi/2)(\sigma_1 + 1)}$.²⁴

In summary, an excited spin-boson model is shown to exhibit novel scattering processes that have a very intuitive explanation. At high enough energies, they are described in terms of Landau-Zener tunneling and eventually lead to the destruction of the composite nature of the polaron. Many aspects of the full quantum-dynamical evolution are lost upon employing the semiclassical or rotating-wave approximations. In particular, the phenomenon of dynamic localization is found to deteriorate due to the entropy-generating quantum corrections described by these scattering processes. These findings have clear, experimentally observable implications regarding many physically interesting situations, such as small polarons in strongly-correlated systems and single atoms in microwave cavities.

This work was supported in part by Natural Sciences and Engineering Research Council of Canada, the Ontario Center for Materials Research, and by the U.S. Department of Energy.

-
- ¹T. Holstein, *Ann. Phys. (N.Y.)* **8**, 325 (1959); **8**, 343 (1959).
²L. Allen and J.H. Eberly, *Optical Resonance and Two-Level Atoms* (Dover, New York, 1987).
³R. Graham and M. Höhnerbach, *Z. Phys. B* **57**, 233 (1984).
⁴D. Feinberg and J. Ranninger, *Physica D* **14**, 29 (1984).
⁵See, for example, V.M. Kenkre and H-L. Wu, *Phys. Rev. B* **39**, 6907 (1989), and references therein.
⁶For example, see J.H. Eberly, N.B. Narozhny, and J.J. Sanchez-Mondragon, *Phys. Rev. Lett.* **44**, 1323 (1980), and references therein.
⁷L. Bonci, P. Grigolini, and D. Vitali, *Phys. Rev. A* **42**, 4452 (1990).
⁸J. Ranninger and U. Thibblin, *Phys. Rev. B* **45**, 7730 (1992).
⁹M.I. Salkola, A.R. Bishop, V.M. Kenkre, and S. Raghavan, *Phys. Rev. B* **52**, R3824 (1995).
¹⁰K. Husimi, *Proc. Phys. Math. Soc. Jpn.* **22**, 264 (1940); K. Takahashi, *Proc. Theor. Phys. Suppl.* **98**, 109 (1989).
¹¹M. Salkola, A. Bishop, S. Trugman, and J. Mustre de Leon, *Phys. Rev. B* **51**, 8878 (1995).
¹²Note that $\vec{\sigma} \cdot \vec{\sigma} = 3$.
¹³K. Takahashi, *J. Phys. Soc. Jpn.* **55**, 762 (1986).
¹⁴We use the presentation in which $\sigma_3 |\pm \frac{1}{2}\rangle = \pm |\pm \frac{1}{2}\rangle$.
¹⁵J. Eiselt and H. Risken, *Phys. Rev. A* **43**, 346 (1991).
¹⁶In this limit, $g \equiv \lambda/\epsilon_0 \rightarrow 0$, which implies that all the polaronic dressing effects vanish as well (Ref. 9).
¹⁷L.D. Landau, *Phys. Z. Sowjetunion* **2**, 46 (1932); C. Zener, *Proc. R. Soc. London Ser. A* **137**, 696 (1932).
¹⁸D.H. Dunlap and V.M. Kenkre, *Phys. Rev. B* **34**, 3625 (1986); G.S. Agarwal and W. Harshwardhan, *Phys. Rev. A* **50**, R4465 (1994); S. Raghavan, V.M. Kenkre, D.H. Dunlap, A.R. Bishop, and M.I. Salkola, *Phys. Rev. E* (to be published); and references therein.
¹⁹L. Bonci, R. Roncaglia, B.J. West, and P. Grigolini, *Phys. Rev. Lett.* **67**, 2593 (1991).
²⁰At the simplest level, we have three kind of oscillations described by the time scales τ_χ (Rabi oscillations), τ_Δ (revivals), and τ_T (tunneling); see Ref. 9.
²¹S.W. McDonald and A.N. Kaufman, *Phys. Rev. Lett.* **42**, 1189 (1979).
²²P. Gaspard, S.A. Rice, and K. Nakamura, *Phys. Rev. Lett.* **63**, 930 (1989).
²³W.-M. Zhang, D.H. Feng, J.-M. Yuang, and S.-J. Wang, *Phys. Rev. A* **40**, 438 (1989).
²⁴H.B. Shore and L.M. Sander, *Phys. Rev. B* **7**, 4537 (1973).